HHS Public Access

Author manuscript

J Invest Dermatol. Author manuscript; available in PMC 2015 April 01.

Published in final edited form as:

J Invest Dermatol. 2014 October ; 134(10): 2531–2540. doi:10.1038/jid.2014.196.

Molecular characterization of human skin response to diphencyprone at peak and resolution phases: therapeutic insights

Nicholas Gulati[1], **Mayte Suárez-Fariñas**[1,2], **Judilyn Fuentes-Duculan**[1], **Patricia Gilleaudeau**[1], **Mary Sullivan-Whalen**[1], **Joel Correa da Rosa**[2], **Inna Cueto**[1], **Hiroshi Mitsui**[1], and **James G. Krueger**[1]

[1]Laboratory for Investigative Dermatology, The Rockefeller University, New York, NY, USA

[2]The Center for Clinical and Translational Science, The Rockefeller University, New York, NY, USA

Abstract

Diphencyprone (DPCP) is a hapten that induces delayed-type hypersensitivity (DTH) reactions. It is used as an immune modulating therapeutic, but its molecular effects in human skin are largely unknown. We studied cellular and molecular characteristics of a recall response to 0.04% DPCP at 3 day (peak) and 14 day (resolution) timepoints using immune markers, RT-PCR and gene array approaches. A peak response showed modulation of ~7,500 mRNA transcripts, with high expression of cytokines that define all major effector T-cell subsets. Concomitant increases in T-cell and CD11c+ dendritic cell (DC) infiltrates were measured. The resolution reaction was characterized by unexpectedly high levels of T-cells and mature (DC-LAMP+) DCs, but with marked decreases in expression of IL-2, IFNγ, and other T-cell derived cytokines. However, negative immune regulators such as IDO1 that were high in peak reactions, continued to have high expression in resolution reactions. In the resolution reaction, ~1,500 mRNA transcripts were significantly different from placebo-treated skin. These data suggest the response to DPCP evolves from an inflammatory/effector peak at day 3 to a more regulated immune response after 14 days. This model system could be useful for further dissection of mechanisms of immune activation or negative immune regulation in human skin.

INTRODUCTION

Haptens like dinitrochlorobenzene and DPCP induce strong DTH recall reactions associated with influx of T-cells and DCs into skin as well as upregulation of an array of inflammatory cytokines during a "peak" response, which ranges from 2-4 days in human skin.(Stute *et al*., 1981) The cellular and molecular events associated with DTH responses in human skin are incompletely understood, especially if one considers that agents like dinitrochlorobenzene

CORRESPONDING AUTHOR: James G. Krueger, Laboratory for Investigative Dermatology, The Rockefeller University, 1230 York Avenue, Box 178, New York, NY, 10065-6399, Ph: 212-327-7730, Fax: 212-327-8232, kruegej@rockefeller.edu.

CONFLICT OF INTEREST: The authors state no conflict of interest.

and DPCP have been used, somewhat paradoxically, to increase local immune responses for the resolution of warts(Upitis and Krol, 2002) and melanoma metastases,(Damian *et al*., 2014) but also to decrease pathogenic immunity for the restoration of hair growth in alopecia areata.(Freyschmidt-Paul *et al*., 2003) One might postulate from these various therapeutic applications that cytotoxic effector immune pathways are induced by topical haptens, while activation of negative regulatory pathways also occurs to eventually down-regulate the inflammatory response. Available data from murine models suggest that resolution of cutaneous immune responses to haptens may be strongly dependent on regulatory T-cells (Tregs) in the skin,(Lehtimäki *et al*., 2012) leading to active mechanisms of immune suppression during the resolution phase of a DTH response. In fact, negative regulatory immune mechanisms may be of more general importance for maintaining skin homeostasis as non-inflammatory in the face of a large population of effector memory T-cells that normally reside in the skin.(Clark *et al*., 2006) The elimination of Tregs from the skin has the consequence of increasing skin inflammation due to environmental or chemical allergens in animal models.(Freyschmidt *et al*., 2010)(Dudda *et al*., 2008) The absence of negative regulatory mechanisms likely contributes to inflammatory skin diseases like psoriasis, where chronic activation of T-cells and DCs, with ongoing production of many inflammatory cytokines, leads to focal plaques of disease that rarely resolve spontaneously.

Cellular and molecular events associated with DTH responses to topical and intradermal antigens are much better understood for the sensitization and early elicitation phases (particularly the peak DTH reaction that occurs within 4 days of recall exposure), compared to later phases of the elicitation response when negative regulatory pathways might be dominant.(Vocanson *et al*., 2009) Very little is known about immune cellular elements and expression of negative regulatory immune molecules during this resolution phase in humans.

In this study, we performed a comprehensive analysis of immune cell types, cytokines defining distinct T-cell subsets in humans, and overall alterations in the skin transcriptome induced during a DTH response to a strong contact allergen (DPCP) in human skin. We defined a peak DTH response as 3 days after DPCP challenge application and a resolution phase reaction as 14 days after application, and profiled reactions at both time points to define cellular and molecular responses during these two phases of the DTH reaction. Our results identified immature myeloid DCs as a major cellular population in the peak response, along with increased synthesis of cytokine transcripts suggestive of pan-T-cell activation. The resolution phase contained a large infiltrate of T-cells and mature [lysosome-associated membrane glycoprotein, dendritic cell-specific (DC-LAMP)+] DCs, as well as dermal Langerin+ cells, along with an altered balance of positive to negative regulatory gene transcripts, suggestive of active immune regulation during this phase of the immune response. We believe the cutaneous DPCP reaction creates a tractable and reproducible system for the future study of positive and negative immune regulation in human skin.

RESULTS

Kinetics of skin inflammation induced by DPCP

Healthy individuals (demographics listed in Table S1) were sensitized to DPCP and two weeks later received two challenge applications on their left thigh and two placebo

applications on their right thigh. Three days after challenge, all subjects exhibited strong clinical inflammation (erythema, induration, and epithelial vesiculation in some cases) only in DPCP-treated sites, whereas placebo-treated sites were indistinguishable from background skin (Figure 1). The clinical DPCP-induced reaction was clearly diminished by 14 days after the challenge dose. Erythema and induration were quantified using a 0-4 scale derived from the Psoriasis Area Severity Index (PASI). The mean response at day 3 was 5.5 (for sum of erythema and induration) and was reduced to 2.1 by day 14 ($p<10^{-7}$) (Table S1). Ultrasound measurements further confirmed a decrease in dermal inflammation over time (Figure 1). Overall, these data support the classical view that 3 days after challenge represents the clinical peak of a DTH response.

Kinetics of cellular and molecular immune response to DPCP in DTH reactions

Biopsies were taken of both DPCP- and placebo-treated sites at day 3 (clinical peak) and at day 14 (resolving inflammation). The first six patients also underwent skin biopsies of reaction sites 4 to 8 months after DPCP challenge (late biopsy). In the acute response, T-cells appeared rapidly at DTH challenge sites with a mean of 1,113 CD3+ T-cells/mm of skin. Overall, T-cell counts diminished slightly by day 14, with a mean of 946 cells/mm. In late biopsies, T-cells were reduced to levels seen in placebo sites (<100/mm). Relative to placebo and generally expected, increases were seen in CD3+ and CD8+ lymphocytes (Figure 2a and b), as well as in DC populations in the day 3 and day 14 biopsies, but two patterns of response were seen with cellular infiltrates as will be discussed in the next section. T-cell activation in biopsies was assessed by RT-PCR measures of mRNAs that are associated with specific T-cell subsets, e.g., IFNγ defining a Th1 response, IL-13 defining a Th2 response, or IL-17 defining a Th17 response (Figure 2c). Marked increases in cytokine mRNA levels occurred in day 3 DPCP-treated sites, with changes ranging from 9-fold to >1000-fold ($\log_2$ 3.2 to >10 as graphed in Figure 2c). The day 14 reactions showed reduced expression of each T-cell subset cytokine with the largest declines in IL-9 and IL-13. All cytokine levels normalized in late biopsies (Figure 2c). The day 3 DPCP response was also associated with a 6-fold increase in forkhead box P3 (Foxp3) mRNA, but this product did not diminish on average in day 14 biopsies. Overall, visible skin inflammation in the DPCP reaction at days 3 and 14 was better correlated with levels of pro-inflammatory cytokine mRNAs than with the number of infiltrating T-cells or DCs. The diminishing production of inflammatory cytokine mRNAs at day 14 with persistence of Foxp3 expression suggests the possibility of an altered positive vs. negative regulatory immune balance in day 3 vs. day 14 reactions.

Molecular profiling of day 3 and day 14 DPCP responses

To profile the global set of gene expression changes in the DPCP reactions, skin biopsies were also hybridized to Affymetrix HGU133 2.0 Plus arrays. A principal components analysis (PCA) of the skin responses is diagrammed in Figure 2d. Day 3 DPCP reactions were widely separated from placebo responses in the major axis of variation (PCA-1), whereas the day 14 reactions approached the placebo sites and late biopsies overlapped completely with placebo responses. Using cutoffs of false discovery rate<0.05 and fold change>2, the day 3 DTH responses had 3,670 upregulated and 3,884 downregulated probesets compared to placebo-treated skin. Tables 1 and 2 list the top ten up-regulated and

down-regulated, respectively, genes in day 3 and day 14 reactions. Since the "top" gene sets are largely different at day 3 vs. day 14, the tables are constructed with a listing of gene expression for both sets of genes at both day 3 and day 14. Among genes with the highest induction at day 3, granzyme B (119-fold increase) and IL-24 (107-fold increase) are molecules with identified roles in tissue rejection or anti-neoplastic control of melanomas or other cancers. Strong expression of CXCL10 (104-fold increase) and CXCL9 (85-fold increase) suggest activation of STAT1-regulated genes by IFNγ production. At day 14, the genes with highest expression at day 3 were strongly down-regulated (on average >10-fold), with IL-24 expression reduced to background levels in placebo-treated skin. In the day 14 biopsies, CCL18 was amplified from the day 3 response and CD1b also became more strongly expressed, likely corresponding to increased DCs at this time point.

The only genes common in top up-regulated products between day 3 and day 14 were defensin beta 4, CXCL10, and S100A9. On a more global level, of the 793 up-regulated and 726 down-regulated probesets at day 14, 317 were uniquely expressed at day 14 and not day 3 (Figure S2a), illustrating that the overall transcriptomic response is distinct between these two time points and that day 14 reactions are not simply an intermediate between day 3 and placebo responses. These unique genes at day 14 included arginase, liver (ARG1), FLT3, and chemokine, C motif, receptor 1 (XCR1) (Table 1c, confirmatory immunohistochemistry and immunofluorescence to co-localize with CD11c+ DCs in Figure S2b and c), all of which may play roles in immune response resolution. In terms of genes that were down-regulated in the DPCP response (Table 2), we noted that the day 3 and day 14 responses were largely distinct, as with up-regulated genes.

The top down-regulated gene at day 3 was IL-37, which is known to negatively regulate inflammatory responses and where ~20-fold increased expression at day 14, relative to day 3, could represent an active regulatory mechanism. A full list of genes that are up-regulated or down-regulated in day 3 and day 14 biopsies is available on request and all microarray data have been deposited in a public database. Granulysin was also highly upregulated (47-fold) and appeared in mononuclear leukocytes in the dermis at days 3 and 14. To localize cells producing granulysin, two color immunofluorescence was performed. The strongest co-localization with granulysin was CD3+ T-cells, with some but not all CD8+ cells staining for this cytolytic effector molecule. A few CD11c+ DCs also appeared to produce granulysin (Figure S3).

Immune infiltrates follow two distinct patterns after a DPCP challenge

In all patients, we measured marked increases in CD3+ T-cells and CD11c+ DCs in day 3 “peak” reactions. However, we detected two distinct reaction patterns for the day 14 “resolution” reaction. One pattern seen in 5/11 patients (subgroup A, Figure 3) showed increasing numbers of T-cells and/or DCs in the day 14 biopsies compared to the day 3 reactions, a response that was entirely unexpected (Figure 3c and d). This subset of patients also showed even larger increases in mature (DC-LAMP+) DCs in day 14 biopsies compared to day 3 biopsies, and this subgroup had the most pronounced dermal infiltrates of Langerin+ cells (Figure 3e and f). However, the expression of inflammation-associated cytokines and CD25 (IL-2RA) usually decreased in day 14 biopsies compared to day 3

reactions, so we detected a disassociation between cellular immune infiltrates and production of inflammatory cytokines/activation molecules (Figure 3a). As further evidence for this, both CD3+ and CD11c+ cell counts did not significantly correlate with gene expression levels of any of the following immune activation markers: IFNγ, IL-2, and IL-2RA (Figure S4). The other response pattern seen in 6/11 patients (subgroup B, Figure S5) fit the expected response kinetics for a DTH reaction: T-cell and DC infiltrates peaked at day 3 and were significantly reduced at day 14 ($p = 0.01$ and 0.001, respectively). As in subgroup A, expression of inflammatory cytokines and activation molecules was decreased in resolution biopsies.

Subjects whose infiltrates decrease from day 3 to day 14 have higher levels of negative regulatory cells and molecules at day 3

We performed immunofluorescence for Foxp3 along with CD3 in order to more specifically identify Tregs which were then quantified as Foxp3+CD3+ cells. On average, subjects in subgroup B had more Tregs than those in subgroup A at day 3 (21.25 versus 9) (Figure 4a and b). We also performed RT-PCR for several known downregulatory molecules. For all molecules tested (IL-10, lymphocyte activation gene 3 (LAG3), programmed cell death 1 (PD1), programmed cell death ligand (PDL) 1, PDL2, IDO1, and CTLA4), mRNA levels were higher at day 3 in subgroup B than subgroup A. Also, there were non-significant but consistent trends for subjects in subgroup B to have higher levels of these molecules even in placebo-treated skin, suggesting baseline immunological differences between subjects in the two subgroups (Figure 4c-i). On a more global level, when looking at a comprehensive list of negative regulator genes (Table S2 has “negative regulator” list, curated through Gene Ontology term 0002683 “negative regulation of immune system process” and literature review, and expression values for DPCP day 3), subjects in subgroup B had higher expression of many of these molecules at day 3 (Figure S6). These data may help explain why subgroup B had decreased cellular infiltrates at day 14 and suggest that different individuals resolve their inflammatory responses to DPCP with different kinetics (inflammation resolution was faster in subgroup B, based on ultrasound measures at days 7 and 14, see Figure S7).

DISCUSSION

This study with DPCP provides the detailed cellular and molecular phenotype of a DTH response at both peak and resolution stages. The strong clinical response at day 3 was accompanied by large increases in infiltrating T-cells and myeloid DCs, as well as by differential regulation (>2 fold change) of 7,555 gene transcripts. The resolution phase was characterized by variable changes in infiltrating leukocytes, overall increased in subgroup A and decreased in subgroup B compared to the peak reaction. In molecular terms, the resolution phase showed decreased expression of T-cell effector cytokines and molecules associated with the activation phase of immune responses, but relatively higher levels of transcripts associated with negative regulation of immune responses. Also, the resolution phase included expression of certain genes including ARG1, XCR1, and FLT3 that were not present during the peak response. ARG1 has been shown to lead to reversible blocks in T-cell proliferation,(Bronte *et al*., 2003) XCR1 contributes to Treg development,(Lei *et al*.,

2011) and FLT3 is involved in maintaining the balance between DC and Treg numbers.(Liu and Nussenzweig, 2010) Although we chose to characterize the immune response to DPCP in normal human skin, our results identify immune mechanisms that may relate to the use of DPCP as an immune modulator in treatment of melanoma or alopecia areata.

In a recent report, 50 patients with cutaneous metastases of melanoma were treated with repeated application of DPCP. Forty-six percent of patients had complete regression of their lesions and a further 38 percent had partial responses, but corresponding study of the immune response to DPCP was not conducted.(Damian *et al*., 2014) The potential of DPCP as an adjuvant to improve immunotherapy has been demonstrated in mice.(von Moos *et al*., 2012) Several immune pathways that we found to be induced by DPCP in normal skin might mediate this anti-melanoma response. First, we identified significant up-regulation of IL-24 mRNA, which is a cytokine with established anti-melanoma activity.(Jiang *et al*., 1995) Since this cytokine was up-regulated only transiently (peak at day 3, but resolved at day 14), it could indicate the need for chronic/repeated application of DPCP to maintain effector cytokines for tumor responses. Furthermore, we observed strong increases in IFNγ expression and this cytokine enhances antigen presentation potential, is anti-proliferative for many cell types,(Braumüller *et al*., 2013) and its induced molecule CXCL10 has anti-melanoma activity.(Antonicelli *et al*., 2011) Another cytokine we found to be upregulated by DPCP, IL-9, has recently been linked to melanoma regression.(Purwar *et al*., 2012) In addition to these cytokines with potential anti-neoplastic effects, DPCP use resulted in many infiltrating CD8+ cells, along with increased granzyme B and granulysin expression, and these would be probable cytotoxic effectors. Granulysin has been shown to promote chemotaxis of CD4+ T-cells in addition to its cytolytic properties,(Deng *et al*., 2005) and both of these functions may contribute to the peak DTH response considering we observed granulysin expression on both CD8+ and CD8- T-cells. We also noted a marked increase in DCs and especially DC-LAMP+ mature DCs, that could provide a local environment to increase antigen presentation of tumor antigens (immature DCs, in the absence of appropriate co-stimulation, present antigens in a tolerogenic fashion), as well as XCR1+ DCs, which have a role in antigen cross-presentation.(Kroczek and Henn, 2012) Overall, this work forms a basis for investigating specific immune elements that may be induced in melanoma lesions that are treated with DPCP as well as the baseline immune competence of cancer patients.

Many different reports have shown that 50-60% of patients with patchy alopecia areata have meaningful hair regrowth when treated with chronic application of DPCP.(Freyschmidt-Paul *et al*., 2003)(Ohlmeier *et al*., 2012) A smaller number of studies have been conducted to investigate immune alterations induced in scalp that is associated with hair regrowth. Identified effects of DPCP include decreasing CD4+ T-cell but increasing CD8+ T-cell infiltrates.(Simonetti *et al*., 2004) Also, MHC class II expression has been shown to be altered by DPCP treatment in different studies, with both increases(Hunter *et al*., 2011) and decreases(Bröcker *et al*., 1987) having been demonstrated. Furthermore, DPCP alters the cytokine profile in treated alopecic scalp, in particular increasing IL-2 and IL-10 expression. (Hoffmann *et al*., 1994) This increased IL-10 expression has been hypothesized to inhibit the lesional T-cells of alopecia areata, and our data confirm an upregulation of IL-10

expression, as well as increases in CD8+ T-cells, in normal human skin treated with DPCP. Our data also suggested roles for various other regulatory molecules in the response to DPCP whose potential relevance to alopecia areata treatment have not yet been elucidated. However, our data do not directly inform on the potential effects of DPCP on scalp tissue as well as alterations which may arise from repeated applications.

We compared our findings on DPCP with those published on a DTH reaction to purified protein derivative (PPD).(Tomlinson *et al*., 2011) The reaction to DPCP at 3 days compared to placebo-treated skin largely encompasses genes that are induced by a specific antigen (PPD in this case, 48 hours after exposure compared to 6 hours) (Figure S8). Of genes that were upregulated in the reactions, 780 were common to PPD and DPCP, but each agent also had unique upregulated genes. Overall there was significant correlation with differentially expressed genes (r=0.61, $p<10^{-16}$) and a gene set enrichment analysis for genes regulated in the PPD reaction had a normalized enrichment score of >4.0, indicating highly similar modulation of gene sets. The analysis of the PPD data by Tomlinson *et al*. emphasized the polar Th1 nature of immune reactions, which is supported by measured increases in IFNγ mRNA, STAT1, and many other interferon-regulated gene products. Without measurement of cytokine production by more sensitive techniques, it is a bit uncertain if other “polar” T-cell subsets are significantly activated by PPD. However, the DPCP response clearly showed activation of all defined “polar” T-cell subsets, i.e., Th1, Th2, Th9, Th17, and Th22, based on cytokine mRNA measures by RT-PCR. Ingenuity Pathway Analysis significantly linked the canonical pathways of “IL-10 Signaling,” “Interferon Signaling,” “IL-6 Signaling,” and “IL-17 Signaling” to the set of genes upregulated in both DPCP and PPD reactions. All of these pathways except for “Interferon Signaling” were also significantly linked to the set of genes uniquely upregulated in DPCP reactions. We feel the system provided here provides a valuable human model for studying DTH reactions, particularly as one does not need to select a subset of antigen-reactive individuals from a larger subset of non-immunized or non-reactive individuals. Also, our system with DPCP controls sensitization and therefore fixes the amount of time between initial antigen exposure and challenge reaction, unlike many alternative antigens.

In contrast to soluble protein antigens, haptens derivatize with proteins that are present in the skin and may thus be present for longer time periods. Hence, different response kinetics might be expected for hapten-induced DTH reactions than PPD reactions. In this study, we did identify an expected inflammatory reaction in the skin that was strong at 3 days after DPCP exposure and T-cell activation, as judged by specific markers (IFNγ, IL-2, and IL-2RA) as well as other activation-associated molecules, was highest at this time point. However, much to our surprise, T-cell infiltrates persisted for much longer than expected based on the PPD model, and 5/11 patients showed increased numbers of T-cells or DCs at day 14 compared to day 3. Also, the number of mature (DC-LAMP+) DCs peaked at day 14 in 7/11 patients. Certainly these data establish a disassociation between T-cell activation/ cytokine production and the magnitude of the cellular immune response defined by the number of T-cells and DCs in the skin. Therefore, the possibility of active negative regulatory mechanisms to suppress T-cell activation to a potentially long-lived cutaneous antigen is suggested by these data.

Overall, understanding the active mechanisms present during the resolution of responses to DPCP could have implications not only for cell-mediated immunity in general, but also for other skin pathologies of either chronic immune activation or ineffective immune responses. Most importantly, this system could provide a tractable human antigen-specific model system for primary discovery of new pathways that may be involved specifically in immune regulation in peripheral tissues. Since all T-cell subsets become activated by *in vivo* DPCP, this system might also have utility to test mechanism/pharmacodynamic actions of new immune modulators designed to selectively inhibit "polar" T-cell subsets or activated T-cells. For example, there has recently been great interest in selective blockade of IL-17 for the treatment of psoriasis and IL-4 for the treatment of atopic dermatitis. As these and many other key cytokines are activated by DPCP, this system can be used to test a variety of pharmacologic agents targeted against pathogenic immune molecules.

MATERIALS AND METHODS

The detailed protocols and statistical analysis are described in Supplementary Materials and Methods online.

Study subjects and skin samples

Skin biopsies of DPCP challenge reactions and placebo-treated sites were obtained from 11 volunteers under a protocol approved by The Rockefeller University's Institutional Review Board. Written, informed consent was obtained from all subjects and the study adhered to the Declaration of Helsinki Principles.

RNA extraction, quantification, and microarray

Total RNA was extracted using the miRNeasy Mini Kit (Qiagen, Valencia, CA) and the amount assessed by NanoDrop 1000 spectrophotometer (Thermo Fisher Scientific Inc., Wilmington, DE). The quality of extracted RNA was examined using Agilent Bioanalyzer 2100 (Agilent Technologies, Palo Alto, CA). RNA was hybridized to HGU133 Plus 2.0 chips (Affymetrix, Santa Clara, CA).

Statistical analysis

Microarray data were analyzed using R/Bioconductor packages (http://www.r-project.org). The data discussed in this publication have been deposited in the National Center for Biotechnology Information's Gene Expression Omnibus (GSE accession number GSE52360, http://www.ncbi.nlm.nih.gov/geo/). Ingenuity Pathway Analysis (www.ingenuity.com) was used to determine canonical pathways significantly linked to various gene sets.

Quantitative RT-PCR

Pre-amplification quantitative RT-PCR technique was used for measuring various genes in total RNA extracted from skin biopsy samples according to the company's instructions.

Immunohistochemistry and Immunofluorescence

Frozen skin sections were prepared and standard procedures were used.

Supplementary Material

Refer to Web version on PubMed Central for supplementary material.

ACKNOWLEDGMENTS

We thank John A. Carucci, Emma Guttman-Yassky, and Michelle A. Lowes for helpful comments and discussions on this manuscript. This research was supported by National Institutes of Health (NIH) grant UL1 RR024143 from the National Center for Research Resources and the Milstein Medical Program. NG was supported by a Medical Scientist Training Program grant from the National Institute of General Medical Sciences of the NIH under award number T32GM07739 to the Weill Cornell/Rockefeller/Sloan-Kettering Tri-Institutional MD-PhD Program. The content of this study is solely the responsibility of the authors and does not necessarily represent the official views of the National Institutes of Health.

ABBREVIATIONS USED

ARG1	arginase, liver
DC	dendritic cell
DC-LAMP	lysosome-associated membrane glycoprotein, dendritic cell-specific
DPCP	diphencyprone
DTH	delayed-type hypersensitivity
Foxp3	forkhead box P3
LAG3	lymphocyte activation gene 3
PCA	principal components analysis
PD1	programmed cell death 1
PDL	programmed cell death ligand
PPD	purified protein derivative
Treg	regulatory T-cell
XCR1	chemokine, C motif, receptor 1

REFERENCES

Antonicelli F, Lorin J, Kurdykowski S, et al. CXCL10 reduces melanoma proliferation and invasiveness in vitro and in vivo. Br J Dermatol. 2011; 164:720–728. [PubMed: 21155750]

Braumüller H, Wieder T, Brenner E, et al. T-helper-1-cell cytokines drive cancer into senescence. Nature. 2013; 494:361–365. [PubMed: 23376950]

Bröcker EB, Echternacht-Happle K, Hamm H, et al. Abnormal expression of class I and class II major histocompatibility antigens in alopecia areata: modulation by topical immunotherapy. J Invest Dermatol. 1987; 88:564–568. [PubMed: 3471816]

Bronte V, Serafini P, Mazzoni A, et al. L-arginine metabolism in myeloid cells controls T-lymphocyte functions. Trends Immunol. 2003; 24:302–306. [PubMed: 12810105]

Clark RA, Chong B, Mirchandani N, et al. The vast majority of CLA+ T cells are resident in normal skin. J Immunol. 2006; 176:4431–4439. [PubMed: 16547281]

Damian DL, Saw RP, Thompson JF. Topical immunotherapy with diphencyprone for in transit and cutaneously metastatic melanoma. J Surg Oncol. 2014; 109:308–313. [PubMed: 24522938]

Deng A, Chen S, Li Q, et al. Granulysin, a cytolytic molecule, is also a chemoattractant and proinflammatory activator. J Immunol. 2005; 174:5243–5248. [PubMed: 15843520]

Dudda JC, Perdue N, Bachtanian E, et al. Foxp3+ regulatory T cells maintain immune homeostasis in the skin. J Exp Med. 2008; 205:1559–1565. [PubMed: 18573908]

Freyschmidt E-J, Mathias CB, Diaz N, et al. Skin inflammation arising from cutaneous regulatory T cell deficiency leads to impaired viral immune responses. J Immunol. 2010; 185:1295–302. [PubMed: 20548030]

Freyschmidt-Paul P, Happle R, McElwee KJ, et al. Alopecia areata: treatment of today and tomorrow. J Investig Dermatol Symp Proc. 2003; 8:12–17.

Hoffmann R, Wenzel E, Huth A, et al. Cytokine mRNA levels in Alopecia areata before and after treatment with the contact allergen diphenylcyclopropenone. J Invest Dermatol. 1994; 103:530–533. [PubMed: 7930677]

Hunter N, Shaker O, Marei N. Diphencyprone and topical tacrolimus as two topical immunotherapeutic modalities. Are they effective in the treatment of alopecia areata among Egyptian patients? A study using CD4, CD8 and MHC II as markers. J Dermatol Treat. 2011; 22:2–10.

Jiang H, Lin JJ, Su ZZ, et al. Subtraction hybridization identifies a novel melanoma differentiation associated gene, mda-7, modulated during human melanoma differentiation, growth and progression. Oncogene. 1995; 11:2477–2486. [PubMed: 8545104]

Kroczek RA, Henn V. The Role of XCR1 and its Ligand XCL1 in Antigen Cross-Presentation by Murine and Human Dendritic Cells. Front Immunol. 2012; 3:14. [PubMed: 22566900]

Lehtimäki S, Savinko T, Lahl K, et al. The Temporal and Spatial Dynamics of Foxp3+ Treg Cell-Mediated Suppression during Contact Hypersensitivity Responses in a Murine Model. J Invest Dermatol. 2012; 132:2744–2751. [PubMed: 22739792]

Lei Y, Ripen AM, Ishimaru N, et al. Aire-dependent production of XCL1 mediates medullary accumulation of thymic dendritic cells and contributes to regulatory T cell development. J Exp Med. 2011; 208:383–394. [PubMed: 21300913]

Liu K, Nussenzweig MC. Origin and development of dendritic cells. Immunol Rev. 2010; 234:45–54. [PubMed: 20193011]

von Moos S, Johansen P, Waeckerle-Men Y, et al. The contact sensitizer diphenylcyclopropenone has adjuvant properties in mice and potential application in epicutaneous immunotherapy. Allergy. 2012; 67:638–646. [PubMed: 22380933]

Ohlmeier MC, Traupe H, Luger TA, et al. Topical immunotherapy with diphenylcyclopropenone of patients with alopecia areata--a large retrospective study on 142 patients with a self-controlled design. J Eur Acad Dermatol Venereol. 2012; 26:503–507. [PubMed: 21569118]

Purwar R, Schlapbach C, Xiao S, et al. Robust tumor immunity to melanoma mediated by interleukin-9-producing T cells. Nat Med. 2012; 18:1248–1253. [PubMed: 22772464]

Simonetti O, Lucarini G, Bernardini ML, et al. Expression of vascular endothelial growth factor, apoptosis inhibitors (survivin and p16) and CCL27 in alopecia areata before and after diphencyprone treatment: an immunohistochemical study. Br J Dermatol. 2004; 150:940–948. [PubMed: 15149507]

Stute J, Hausen BM, Schulz KH. [Diphenylcyclopropenone - a new strong contact sensitizer (author's transl)]. Dermatosen Beruf Umw Occup Environ. 1981; 29:12–14.

Tomlinson GS, Cashmore TJ, Elkington PTG, et al. Transcriptional profiling of innate and adaptive human immune responses to mycobacteria in the tuberculin skin test. Eur J Immunol. 2011; 41:3253–3260. [PubMed: 21805471]

Upitis JA, Krol A. The use of diphenylcyclopropenone in the treatment of recalcitrant warts. J Cutan Med Surg. 2002; 6:214–217. [PubMed: 11951129]

Vocanson M, Hennino A, Rozières A, et al. Effector and regulatory mechanisms in allergic contact dermatitis. Allergy. 2009; 64:1699–1714. [PubMed: 19839974]

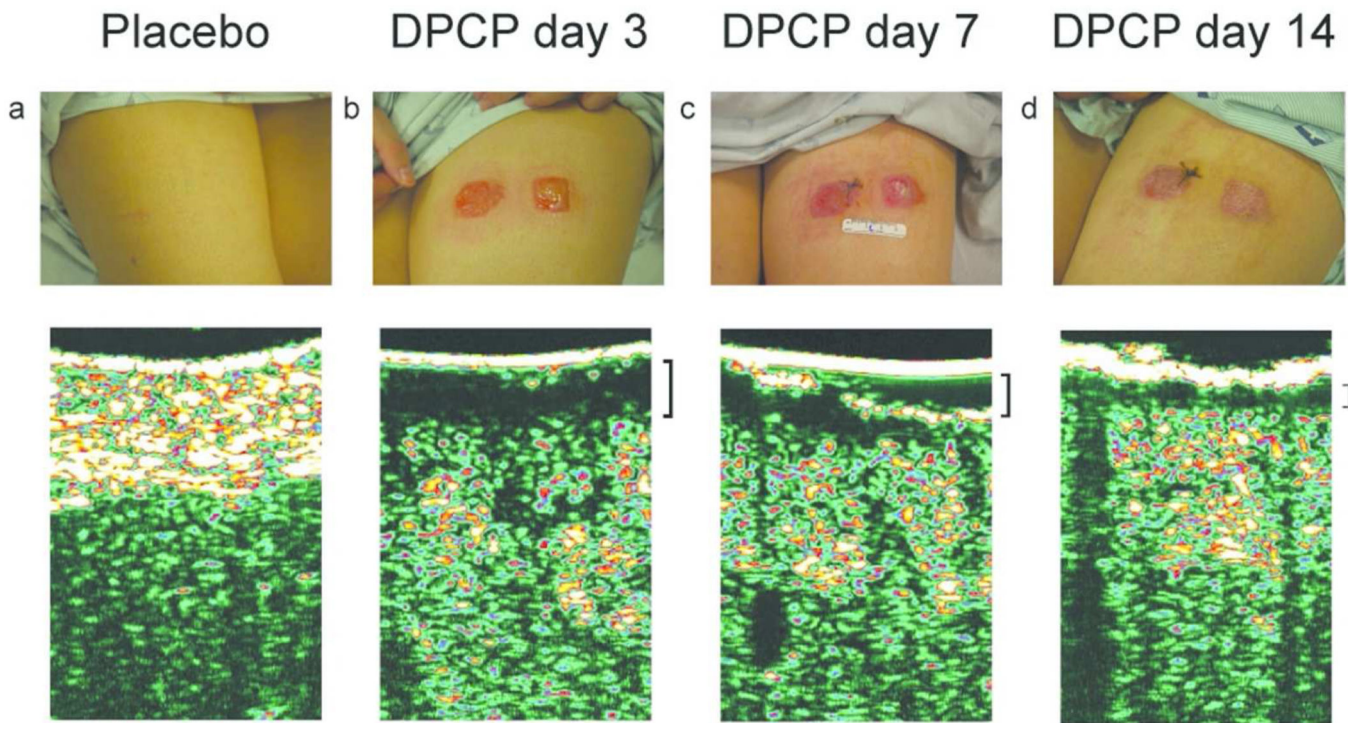

Figure 1.

Visualization of inflammatory reactions induced by DPCP over time. Clinical photography with ultrasound imaging below of a skin site (a) treated with placebo, (b) 3 days after treatment with DPCP, (c) 7 days after treatment with DPCP, and (d) 14 days after treatment with DPCP. Brackets on ultrasound images indicate extents of inflammatory reactions as reflected by dermal thickness. Shown is a representative subject (subject 008).

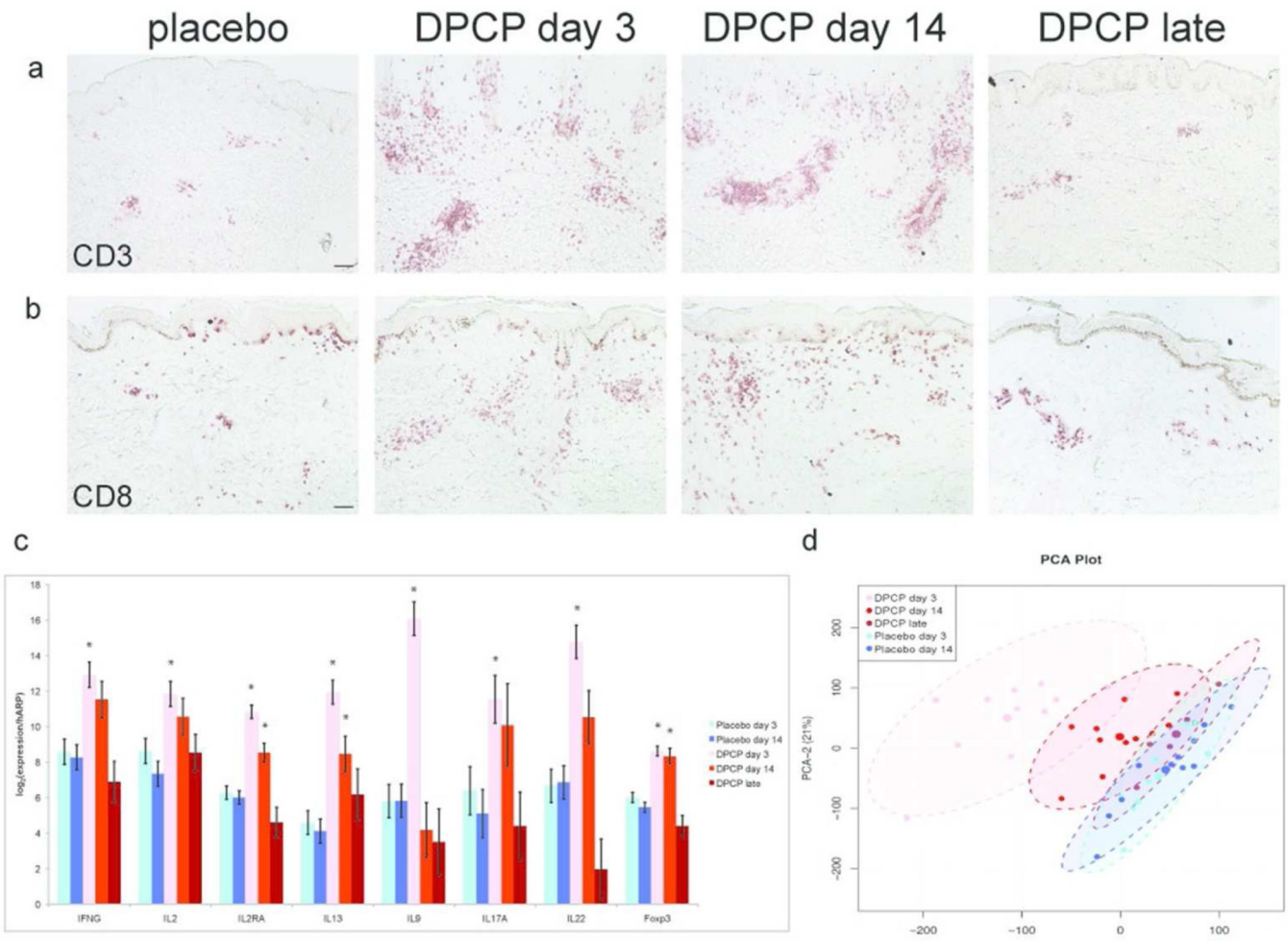

Figure 2.

Reactions to DPCP include immune activation markers that are present at day 3 but diminish over time. (a, b) Immunohistochemistry for CD3 (a) and CD8 (b) on placebo-treated samples, DPCP day 3 samples, DPCP day 14 samples, and DPCP late samples. Scale bar = 100 μm. (c) RT-PCR analysis for IFNγ, IL-2, IL-2RA, IL-13, IL-9, IL-17A, IL-22, and Foxp3. Shown are average normalized expression values for placebo-treated day 3 samples (light blue bars, n=11), placebo-treated day 14 samples (dark blue bars, n=11), DPCP day 3 samples (pink bars, n=11), DPCP day 14 samples (red bars, n=11), and DPCP-treated samples 4-8 months after challenge (late) (brown bars, n=6). Asterisks indicate $p<0.01$ when compared to placebo and error bars represent standard errors of the mean. (d) Principal components analysis (PCA) of microarray data showing all samples as individual dots colored according to sample type. The larger dots are averages for each sample type.

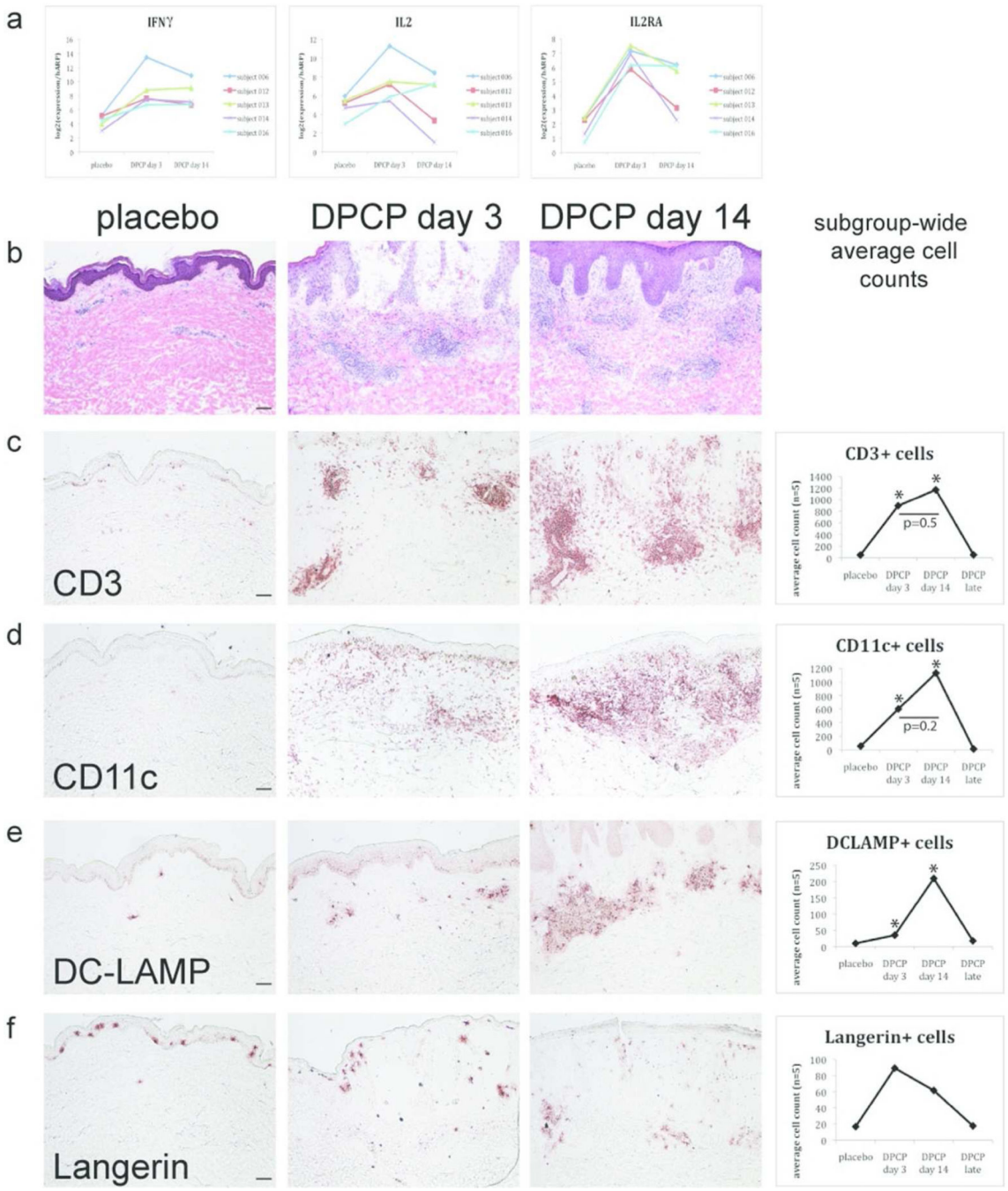

Figure 3.

RT-PCR and histological analysis of subjects whose CD3+ or CD11c+ infiltrates increase from 3 days to 14 days post-DPCP challenge (subgroup A, n=5). (a) RT-PCR analysis for IFNγ (left panel), IL-2 (middle panel), and IL-2RA (right panel). Shown are normalized expression values for each subject individually to highlight that almost all samples have decreased expression of these genes at day 14 compared to day 3. (b-f) H&E (b) and immunohistochemical analysis of samples for (c) CD3, (d) CD11c, (e) DC-LAMP, and (f) Langerin. For all histological images, left panels show placebo reactions, middle panels

show DPCP day 3 reactions, and right panels show DPCP day 14 reactions. Shown is a representative subject (subject 013). For immunohistochemical stains, line graphs indicate subgroup-wide average cell counts for placebo, DPCP day 3, DPCP day 14, and DPCP late samples. Asterisks indicate $p<0.05$ when compared to placebo. Scale bar = 100 μm.

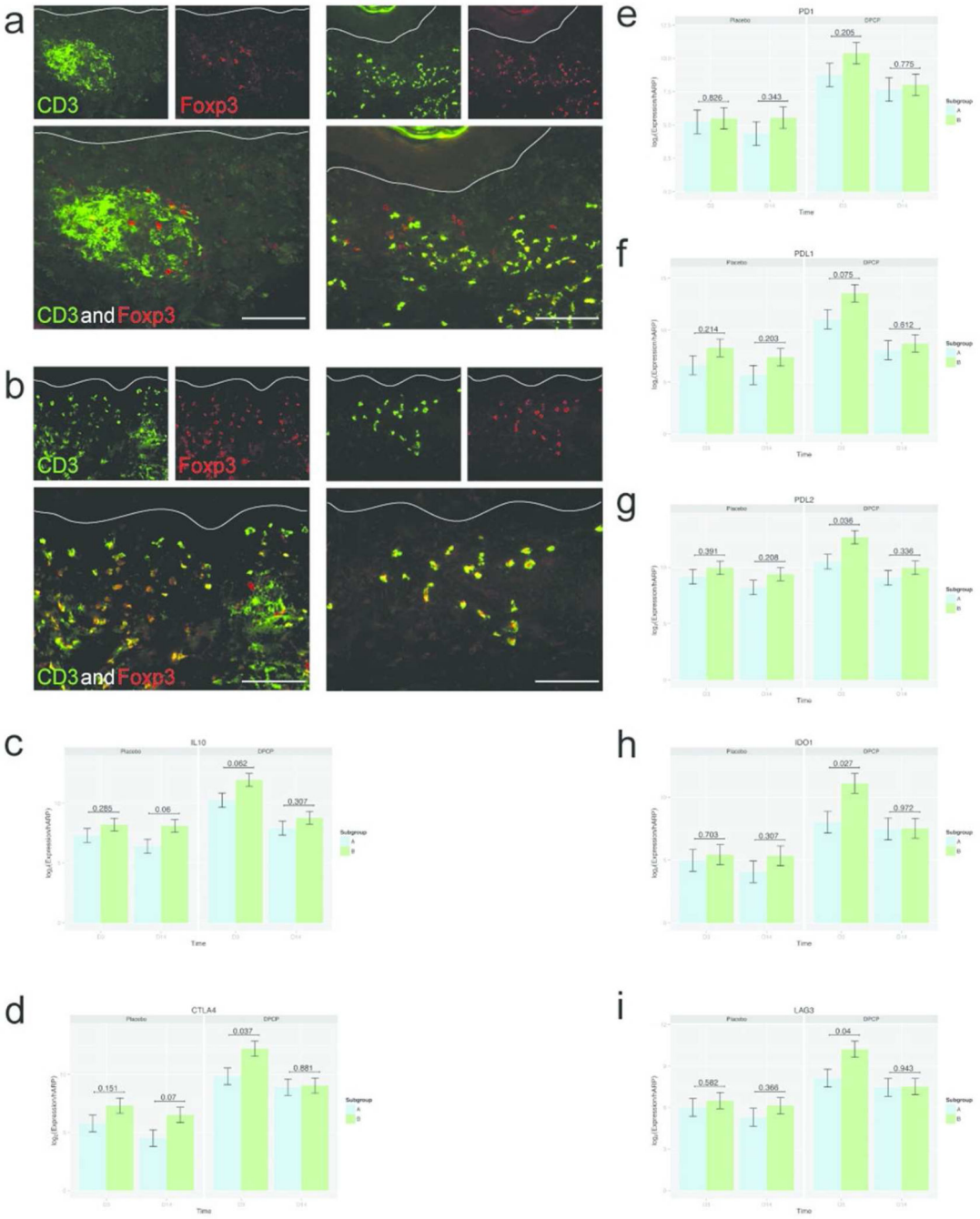

Figure 4.

Negative regulatory immune cells and molecules are increased in DPCP day 3 reactions of subgroup B compared to subgroup A. (a, b) Foxp3 (red)-CD3 (green) immunfluorescence for (a) a representative subgroup A member (subject 012) and (b) a representative subgroup B member (subject 021). Left panels are DPCP day 3 samples and right panels are DPCP day 14 samples. Tregs were quantified as double-positive for Foxp3 and CD3. Subject 012 had 4 double-positive cells at day 3 (subgroup-wide average of 9) and 24 at day 14 (subgroup wide average of 20.33) while subject 021 had 37 at day 3 (subgroup-wide average

of 21.25) and 19 at day 14 (subgroup-wide average of 12). (c-i) RT-PCR analysis for (c) IL-10, (d) CTLA4, (e) PD1, (f) PDL1, (g) PDL2, (h), IDO1, and (i) LAG3. Shown are average normalized expression values of placebo day 3, placebo day 14, DPCP day 3, and DPCP day 14 skin for both subgroups (n=5 for subgroup A (blue bars), n=6 for subgroup B (green bars)). *p*-values are shown to compare subgroup A with subgroup B for each sample type. Scale bar = 100 μm.

Table 1

Top 10 up-regulated genes in DPCP day 3 and DPCP day 14 vs placebo samples

Gene	Description	fold change at day 3	fold change at day 14
(a) top up-regulated transcripts at day 3			
SERPINB4	serpin peptidase inhibitor, clade B (ovalbumin), member 4	340.5	10.6
S100A7A	S100 calcium binding protein A7A	170.9	6.1
DEFB4A	defensin, beta 4A	169.5	17.0
MMP1	matrix metallopeptidase 1 (interstitial collagenase)	167.3	4.9
MMP12	matrix metallopeptidase 12 (macrophage elastase)	147.9	8.4
GZMB	granzyme B (granzyme 2, cytotoxic Tlymphocyte-associated serine esterase 1)	118.8	11.2
IL24	interleukin 24	106.8	1.3
CXCL10	chemokine (C-X-C motif) ligand 10	104.2	25.5
S100A9	S100 calcium binding protein A9	97.7	15.7
APOBEC3A	apolipoprotein B mRNA editing enzyme, catalytic polypeptide-like 3A	95.0	1.2
(b) top up-regulated transcripts at day 14			
CXCL9	chemokine (C-X-C motif) ligand 9	84.7	37.3
COL6A6	collagen, type VI, alpha 6	11.0	36.1
CCL18	chemokine (C-C motif) ligand 18 (pulmonary and activation-regulated)	15.0	32.1
CXCL10	chemokine (C-X-C motif) ligand 10	104.2	25.5
SERPINB3	serpin peptidase inhibitor, clade B (ovalbumin), member 3	68.0	23.3
COL6A5	collagen, type VI, alpha 5	15.8	20.1
CD1B	CD1b molecule	10.5	19.6
DEFB4A	defensin, beta 4A	169.5	17.0
S100A9	S100 calcium binding protein A9	97.7	15.7
OASL	2'–5'-oligoadenylate synthetase-like	54.5	12.1
(c) regulatory genes with selective expression in day 14 samples			
ARG1	arginase, liver	0.2	11.6
FLT3	fms-related tyrosine kinase 3	2.5	11.5
XCR1	chemokine (C motif) receptor 1	0.3	6.1

Table 2

Top 10 down-regulated genes in DPCP day 3 and DPCP day 14 vs placebo samples

Gene	Description	fold change at day 3	fold change at day 14
(a) top down-regulated transcripts at day 3			
IL37	interleukin 37	−46.0	−2.3
ATP1A2	ATPase, Na+/K+ transporting, alpha 2 polypeptide	−38.3	−3.2
GDF10	growth differentiation factor 10	−36.4	−3.2
SGCG	sarcoglycan, gamma (35kDa dystrophin-associated glycoprotein)	−29.8	−4.4
MYOC	myocilin, trabecular meshwork inducible glucocorticoid response	−29.2	−7.1
VIT	vitrin	−26.8	−2.7
DPP6	dipeptidyl-peptidase 6	−25.6	−3.2
THRSP	thyroid hormone responsive	−24.9	−3.4
DLG2	discs, large homolog 2 (Drosophila)	−23.7	−1.4
FIBIN	fin bud initiation factor homolog (zebrafish)	−23.4	−4.7
(b) top down-regulated transcripts at day 14			
WIF1	WNT inhibitory factor 1	−6.2	−27.1
GALNTL2	UDP-N-acetyl-alpha-D-galactosamine:polypeptide N-acetylgalactosaminyltransferase-like 2	−2.1	−9.9
RBP4	retinol binding protein 4, plasma	−10.8	−8.2
BTC	betacellulin	−19.8	−8.1
LEP	leptin	−7.2	−8.0
TNMD	tenomodulin	−10.2	−7.8
MYOC	myocilin, trabecular meshwork inducible glucocorticoid response	−29.2	−7.1
MUC7	mucin 7, secreted	−5.6	−6.1
IL17D	interleukin 17D	−13.6	−6.1
SPINK1	serine peptidase inhibitor, Kazal type 1	−3.4	−5.9